

Single Pulse Jet Impingement on Inclined Surface, Heat Transfer and Flow Field

2013-24-0003

Published
09/08/2013

Mirko Bovo
Chalmers University / Volvo Cars

Borja Rojo
Chalmers University

Copyright © 2013 SAE International
doi:10.4271/2013-24-0003

ABSTRACT

This paper focuses on the heat transfer and flow field resulting from a single pulse impinging jet. The size, time scale and jet characteristics are relevant to automotive diesel injection process. The purpose is to study jet impingement by correlating and cross comparing different measurements and simulations of the same event. The pulse jet impinges on a flat surface at different angles (0° , 30° , 45° , 60°) and a 90° rounded edge.

Experiments are performed deploying various techniques to record the event; PIV for the flow field, high acquisition rate thermocouples and infrared camera for surface temperature. The cases are reproduced with CFD simulations including conjugated heat transfer. The flow is simulated using LES.

The results highlight that the jet penetration rate is a function of the target angle. Also, the heat transfer magnitude and space distribution depends on the surface inclination. Alongside, the consistency of the results validates CFD as a powerful tool to study this type of flow.

INTRODUCTION

Jets are interesting flows found in many natural and industrial environments. A good review of imping gas jet is [1] and [2] extends the work for flame jets. Impinging jets are known for their high levels of heat transfer, they have been studied in a number of configurations varying in geometrical and dynamic parameters. The historic references for impinging jet heat transfer is [3] and for the flow field [4], since then much

work has been carried out, A number of experimental investigation using different techniques and jet configurations can be found in [5, 6, 7, 8, 9, 10, 11]. Impinging jets are known to be difficult to model and predict and are indeed a recommended test case for turbulence models [3]. Different numerical approaches to model stationary impinging jets are extensively studied in literature [12, 13, 14, 15, 16, 17, 18]. A work by the author collects, repeats and reviews many of these models from an engineering point of view [19].

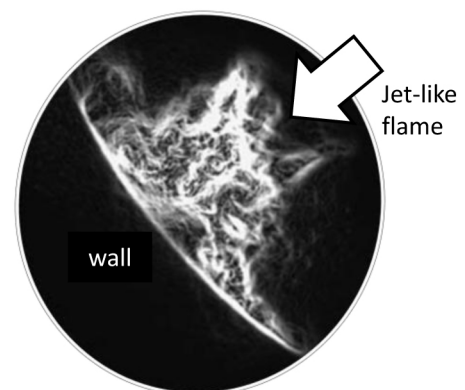


Figure 1. Pictures of diesel injection - combustion obtained with endoscopy technique in a working heavy duty engine. Clearly visible the jet-like flame impinging on the combustion chamber wall. Courtesy of [20]

In many cases the jet is not stationary (i.e. continuous) but it is delivered as a pulse. One such case is the fuel injection in diesel engines. At every power stroke a spray of fuel is injected into the combustion chamber resulting in a jet-like

pulse impinging on the chamber wall [20]. In most cases, the jet impinges on the piston surface with changing angles due to the piston's shape and motion.

Much experimental work is carried out on spray liquid and vapor penetration, which is essential on the study of Internal Combustion Engines (ICE) [21, 22, 23]. Results on this field show that an evaporating-combusting spray shares many features with jets. Modelling of the injection process is also focus of considerable research [24, 25, 26, 27, 28], some of which is based on the equivalent jet assumption to describe the gas motion generated by the spray. However, the work focuses mainly on the free spray/jet and little material is found on the event of a pulse jet approaching a wall with emphasis on heat transfer (i.e. single pulse impinging jet).

Work on pulsating impinging jet is found related to the cooling of electronic components. In these cases the material found is characterized by multiple pulsations [29, 30, 31, 32] but none with characteristic similar to the ICE injection process.

In this work we investigate the heat transfer and flow field caused by a single pulse impinging jet with characteristics relevant to ICE application. The work is based upon measurements with three experimental techniques and a series of numerical simulations. The emphasis is placed on describing the flow features and thermal effects of the impinging jet in different geometrical configurations. For this reason the measurements techniques and simulations details are only presented briefly.

THE CASE AND ITS RELEVANCE

The primary purpose of the experimental campaign is to collect data on pulse jet impingement for a meaningful comparison with the CFD (Computational Fluid Dynamics) simulation. For this reason the flow is measured with various techniques to capture the jet velocity field and the thermal effects on the impingement wall. The flow field is measured with PIV (Particle Image velocimetry). The jet-wall thermal interaction is measured with fast responding thermocouples and infrared thermal camera. These different techniques allow resolving the event with high degrees of precision in time and space respectively.

This work is oriented towards the injection process in automotive diesel engines. Diesel injection event includes a number of phenomena such as liquid injection, spray break-up, vaporization, air entrainment/mixing, self-ignition, combustion and wall impingement. This is a multi-physics event challenging to understand, measure and model. One way to tackle such complex event is to isolate the different physical phenomena and understand them separately, subsequently the mutual interaction can be taken into account step by step. For this reason there is an amount of specific work, for example, on spray break-up [28] or comparing flow feature between ignited and non-ignited spray/jets [34]. The wall impingement phase is a late part of the process and thus

depends upon all events occurring upstream making it impractical to study directly.

The priority of this work is to measure the same event with high accuracy and multiple measuring techniques. For this reason the case is drastically simplified with care not to lose the characteristic features of the reference case (ICE diesel injection). Following, the simplifications are explained one by one.

A high pressure gas jet is used instead of the diesel spray. In the vast majority of the cases the flow reaching the combustion chamber wall is fully evaporated. This can be seen on the studies presenting the liquid and gas penetration length such as [23]. Consequently the flow is very similar to a reacting gas jet. For this reason a number of models for diesel spray are based on the equivalent jet analogy, for example [27]. What characterizes a jet is mainly its momentum, indeed travelling downstream, a jet entrains fluid from the surrounding but conserves its momentum, with exclusion of the viscous losses, as explained in basic fluid mechanics [35]. The velocity profile of the gas jet used in the experiment is compared with the evaporated spray at the same distance from the wall showing high similarity Figure 2. The velocity is measured with PIV technique while the diesel spray is modeled by [28] for a typical automotive application. The simulation confirms also that the spray is fully evaporated at this location.

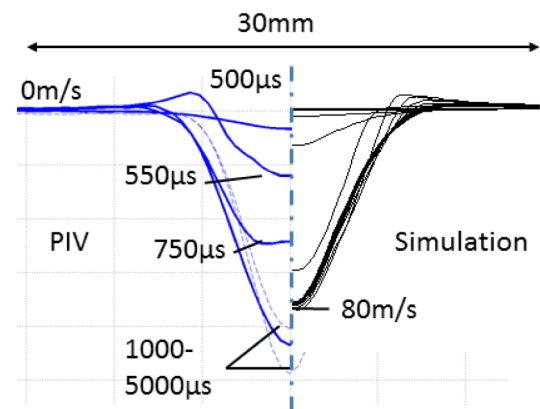


Figure 2. Comparison between PIV measurements of the gas jet used and Diesel spray simulation. Location: 20mm from the target. Diesel spray fully evaporated, non-ignited [28].

The jet-like flame impinging on the combustion surface is a reacting flow. The chemical processes change the enthalpy of the flow. This largely affects the temperature field but experiments show that the effect on the jet velocity is not drastic [33]. On the other hand, the presence of the wall strongly affects the combustion process as, for example, indicated by [34] but this is out of the scope of this work.

The gas jet is at room temperature and the experiment is run at standard room conditions. Temperature and pressure are very important variables which have radical effects on the

fluid properties (e.g. density and viscosity). However, it is straight forward to include these variables in a CFD simulation since these phenomena are very well understood and can be described by thermodynamic laws. Therefore, results from this case can be easily transferred to the combustion chamber environment. On the other hand, working at room conditions greatly facilitates the access to the event to be measured and ease the execution of high precision measurements with multiple techniques.

In the experiment a jet at room temperature impinges on a hot surface hence the heat flux is inverted compared to diesel ICE (high temperature jet-like flame on combustion chamber wall). Also, the experimental configuration gives raise to natural convection phenomena but these are estimated to be two orders of magnitude smaller than the impinging jet in terms of heat transfer.

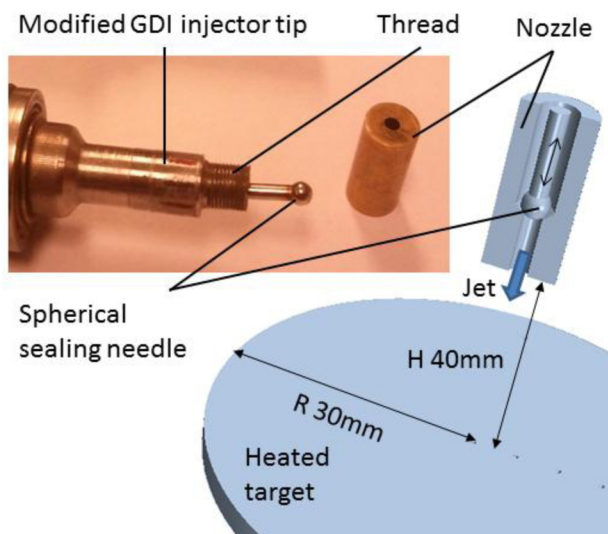


Figure 3. Description of the experimental setup. Details of the modified GDI (Gasoline Direct Injection) injector and nozzle-target relative positioning.

The gas jet is generated by a modified gasoline DI injector (Figure 3) inspired by [36]. The nozzle is a 1mm diameter, 6mm long hole sealed by a needle with spherical tip. The fluid used is synthetic air. The conditions upstream the needle are 10bar and 20C. The jet is discharged in quiescent air at atmospheric conditions, in these conditions the jet is under-expanded. A description of this type of flow can be found in [36]. The flow is supersonic at the nozzle but rapidly becomes subsonic through a series of expansion shock waves. This study focuses only on the region downstream the transition region. The jet is directed to an aluminum plate at 150C. The target is at 40mm from the nozzle. The injection duration is 5ms and the jet is fully developed after ~1ms from start of injection (Figure 2). A reference Re of ~90000 is associated to the fully developed jet. Re is calculated upon the approximate width of the jet and the jet peak velocity 20mm from the impingement wall. From start of injection the jet takes about 0,75ms to reach the target with an average velocity of 40m/s.

Modern diesel pistons have a bowl-like shape to improve the combustion process (see the example in Figure 4). The shape function is very complex acting on the swirl motion of the compressing air and on the development of the jet-like flame during the first part of the combustion. De facto, the jet hits the walls of the piston at different angles due to the piston motion as schematically shown in Figure 4. For this reason the targets in the experiment are chosen to be: 1) A flat plate inclined at different angles. 2) A rounded 90 degrees corner with a 5mm radio (Figure 4 bottom).

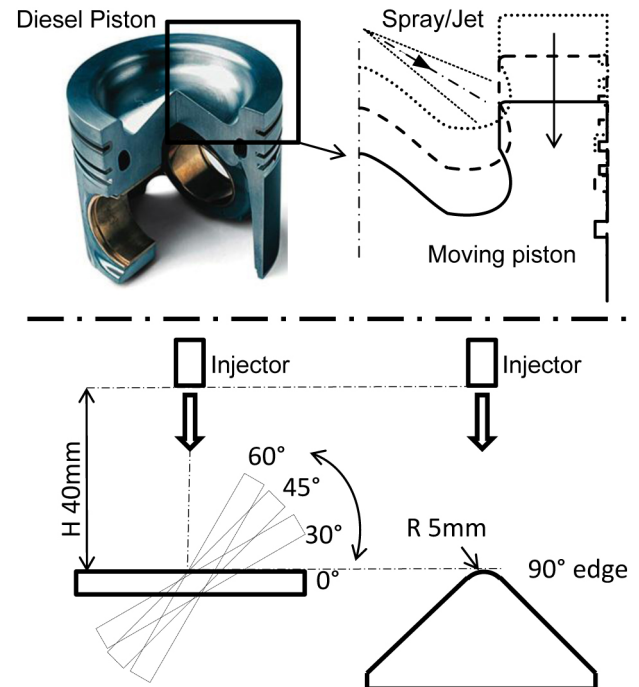


Figure 4. Top, example of modern diesel piston geometry. Bottom, experiment target positioning relative to the injector.

MEASUREMENTS TECHNIQUES

PIV (Particle Image Velocimetry)

PIV is a well-established technique to measure flow velocity. The experiment has been carried out closely following the methodology presented in [37]. PIV is used to measure instantaneous velocity field at different times. The flow is seeded with cigarette smoke. The smoke particle size is checked with an electrical mobility measurement apparatus. The smoke consists of a high concentration 80 - 100nm particles, their size and density are appropriate to follow the jet flow in the subsonic region. The cigarette is located in a ~1dm³ vessel fed with synthetic air. From the vessel a short line feeds the injector. This results in a readily available, standardized and cheap solution for seeding high-pressure/low-mass-flow systems.

The PIV system allows for a fine resolution of the instantaneous jet flow in space. Limitations in the system acquisition rate allow only for one acquisition per jet, hence it

is not possible to follow the evolution in time of the same jet event. This can only be done on the average values.

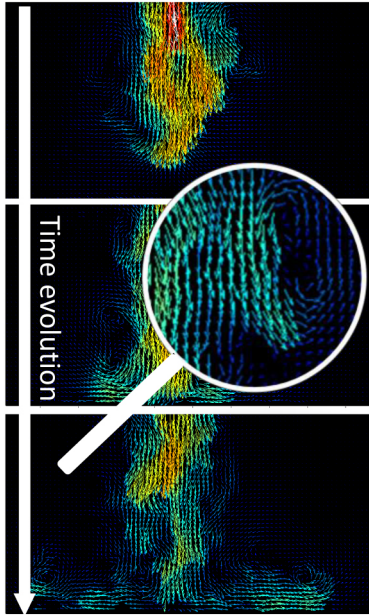


Figure 5. Example PIV results (note: the pictures are uncorrelated, i.e. not the same jet event).

The shear effect between the jet front and the surrounding creates vortices clearly visible in [Figure 5](#) and [Figure 6](#). These structures are slower than the jet and are left behind contributing to the formation of the shear layer. In the figures zoom-ins [Figure 5](#) it is also possible to appreciate the magnitude of the turbulent structures. The jet to jet variation is significant. As a result, in the average results ([Figure 7](#)) the turbulent structures are less sharp but still clearly visible. This implies that the primary vortex structures are consistent and repeatable.

The jet penetration velocity changes with the target angle (Compare the pictures of column 0,75ms in [Figure 7](#)). This indicates that the presence of the target affects the evolution of the free jet plume. The jet needs to push away the quiescent air to reach the target surface. This process is facilitated if the target is inclined. Accordingly, the steeper the angle the faster the jet penetration.

Comparing [Figure 7](#) at time 2ms it is visible that the case at 0° has a symmetrical development. In the case 30° a vortex can be seen climbing upwards. This is smaller and slower than the vortex travelling downwards. For the case at 60° the upward travelling vortex is not visible. Moreover, the downwards moving vortex is larger and travels faster compared to the 30° case.

Thermocouples

The flat target is equipped with eight thermocouples placed at the surface in the impingement area ([Figure 8](#)). The thermocouple construction and characteristics can be found in [\[38\]](#). The sensing element is the junction between the first

and second thermocouple element and it is realized with a thin layer of vaporized metal deposited under vacuum as shown in [Figure 8](#). The result is a device with very low thermal inertia capable to respond to temperature changes of the surrounding within μs , hence capable to accurately resolve the impingement event. Six thermocouples are placed in a row 5mm apart thus able to time resolve the radial effect of the jet. Further, two thermocouples are placed at $R=25\text{mm}$ providing information about the axial-symmetry of the jet.

The results for the thermocouple experiment are reported in [Figure 9](#). The highest heat transfer rate is measured at $R=0\text{mm}$ with the target at 0° . For the cases at 60° the highest heat transfer is measured at $R=5\text{mm}$ upwards indicating that the location of the stagnation point shifts with increasing angle. The jet effect rapidly decreases in the upward direction with practically no effect for the case 60° at $R=20\text{mm}$. All cases with inclined target have similar measurements on the downward direction ([Figure 9](#) red lines), matching the results for 0° case at $R=15\text{mm}$. The graphs show the entire duration of the injection, including part of the pre jet and post jet conditions. From the results it is possible to estimate the velocity of the wall-jet. This takes 2 to 3ms to reach the thermocouple at $R=20\text{mm}$ depending on the inclination and direction (upward or downward).

Thermal Camera

The target temperature is measured with a thermal camera rigged as show in [Figure 10](#). The setup is carried out as described in [\[39\]](#). The accuracy in the temperature range of interest is $\sim 0.1\text{C}$. The image integration time is 0.5ms, thus the jet (5ms) is resolved with about 10 frames. This rate is achievable by reducing the frame size to 64×12 pixels. In turns, this leads to a resolution in space of $\sim 1\text{mm}$. The surface is painted with a $\sim 50\mu\text{m}$ layer low emissivity black paint with characteristics described in [\[39\]](#). This paint layer is thick enough to have a significant thermal insulation effect.

Consequently, only the time response and space distribution can be directly compared to the thermocouple experiment but not the magnitude of the temperature variation.

An example of the results is given in [Figure 11](#), here is possible to see also that the target center is marked for geometrical reference (blue dots). [Figure 12](#) top presents the average of 20 samples for the thermal camera measurements in the line across the stagnation point. At time 1ms all cases detect an interaction between the jet and the surface, notably the steeper the angle the stronger the effect. This indicates that the jet reaches the target earlier with an inclined target. The thermal effects are expected to be highest for the case at 0° , consistently this case has the highest temperature change in the time 1 to 5ms. In the cases with an inclination the results are asymmetrical. For the cases with 45° and 60° the jet effect never reaches the highest part of the target resulting in no temperature variation from the initial conditions. The temperature distribution for the case at 0° is symmetrical during the whole event and presents the highest standard

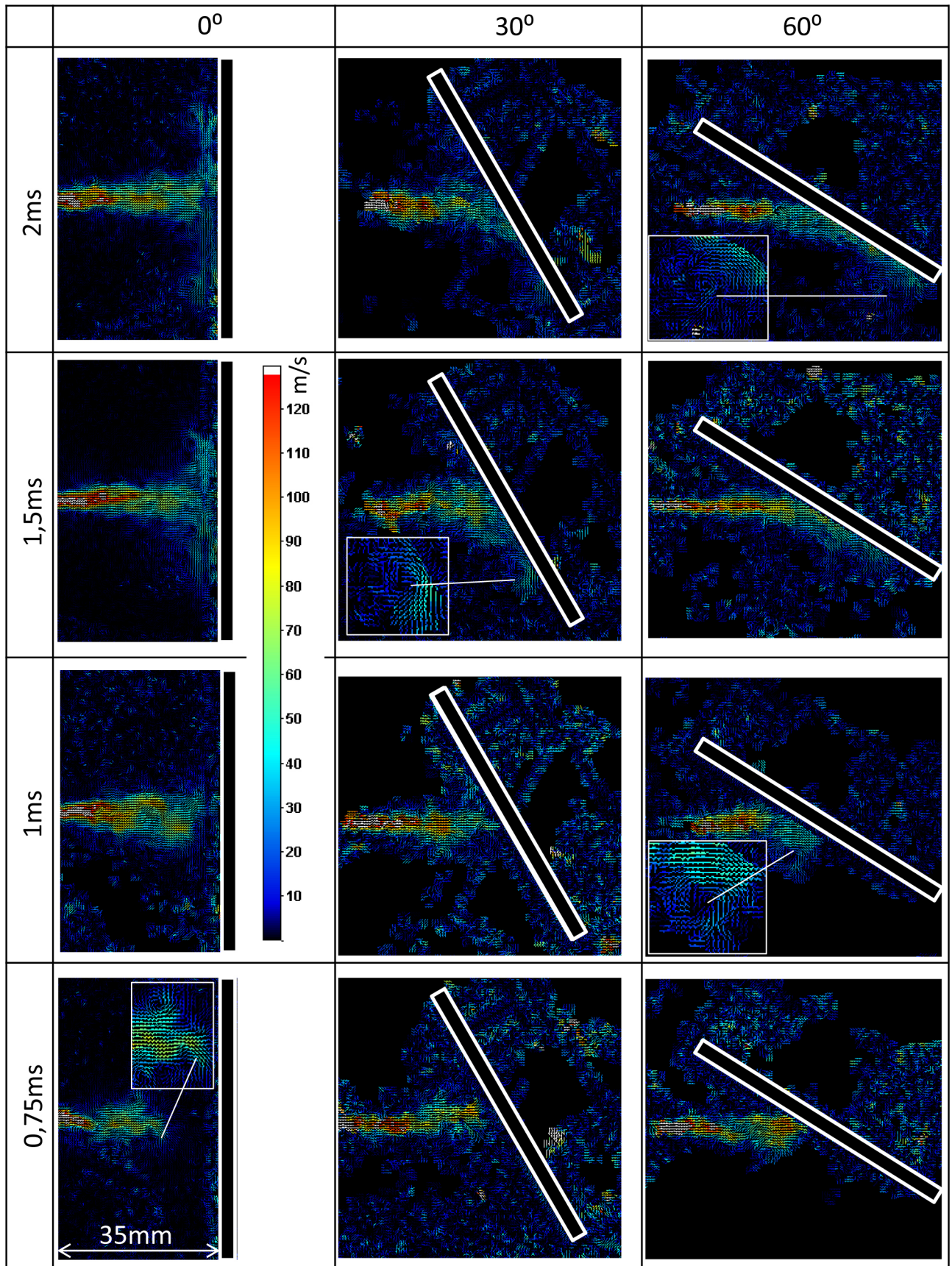


Figure 6. PIV results instantaneous. Selected zoom-in of the vortices in white frame.

deviation (Figure 12 bottom) indicating a high jet to jet variation.

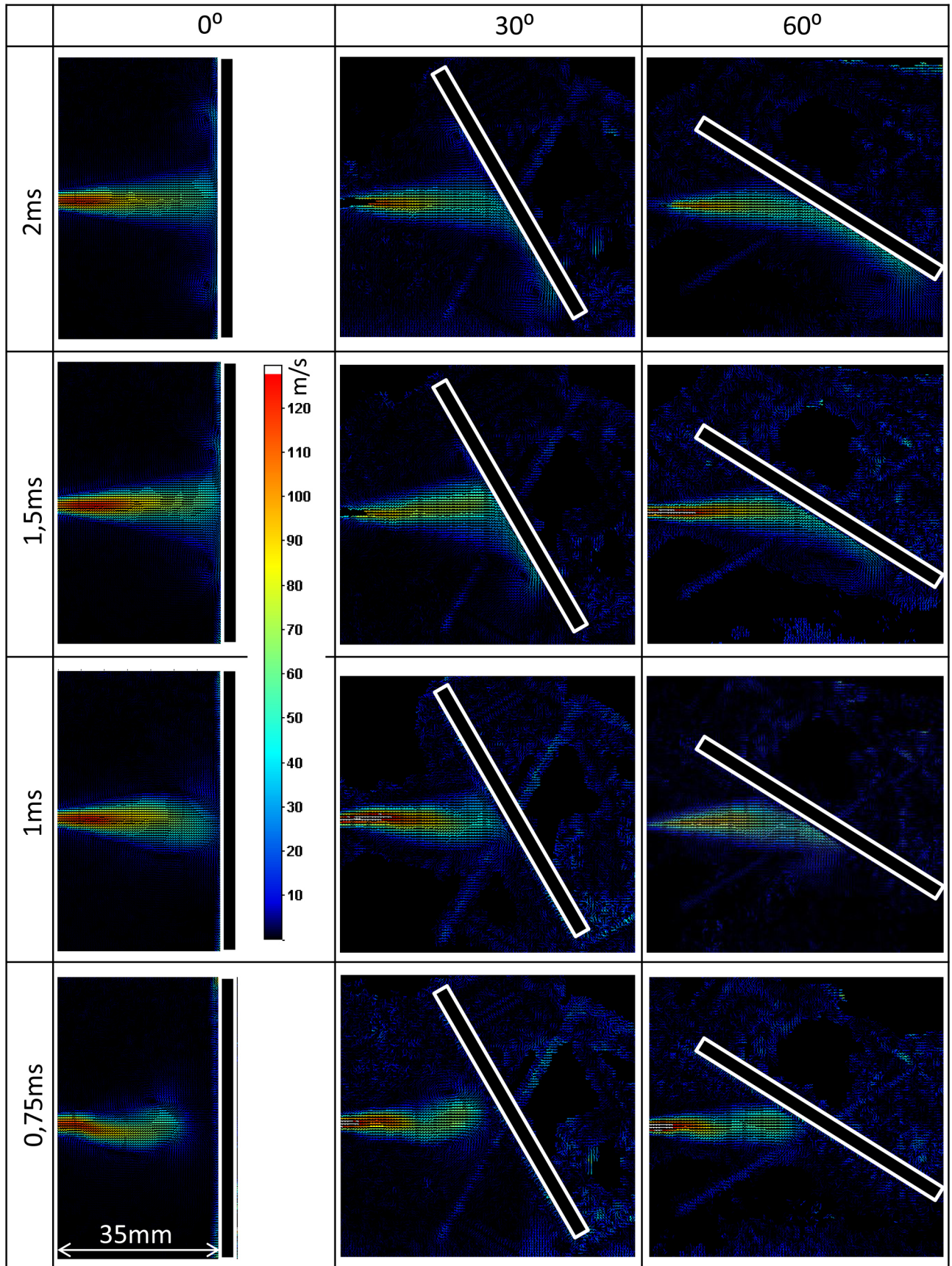


Figure 7. PIV results average. Average of 100 samples.

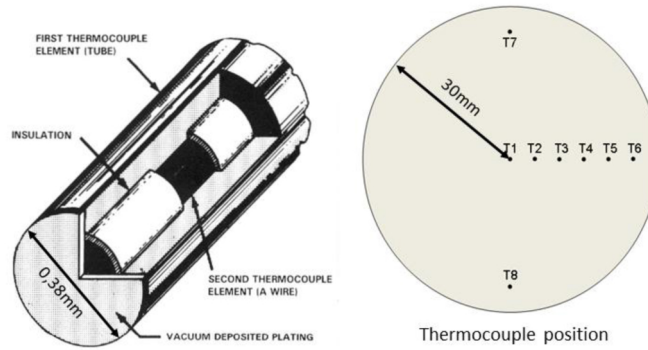


Figure 8. Left. Thermocouples construction details [38]. Right. Thermocouples positioning on the target.

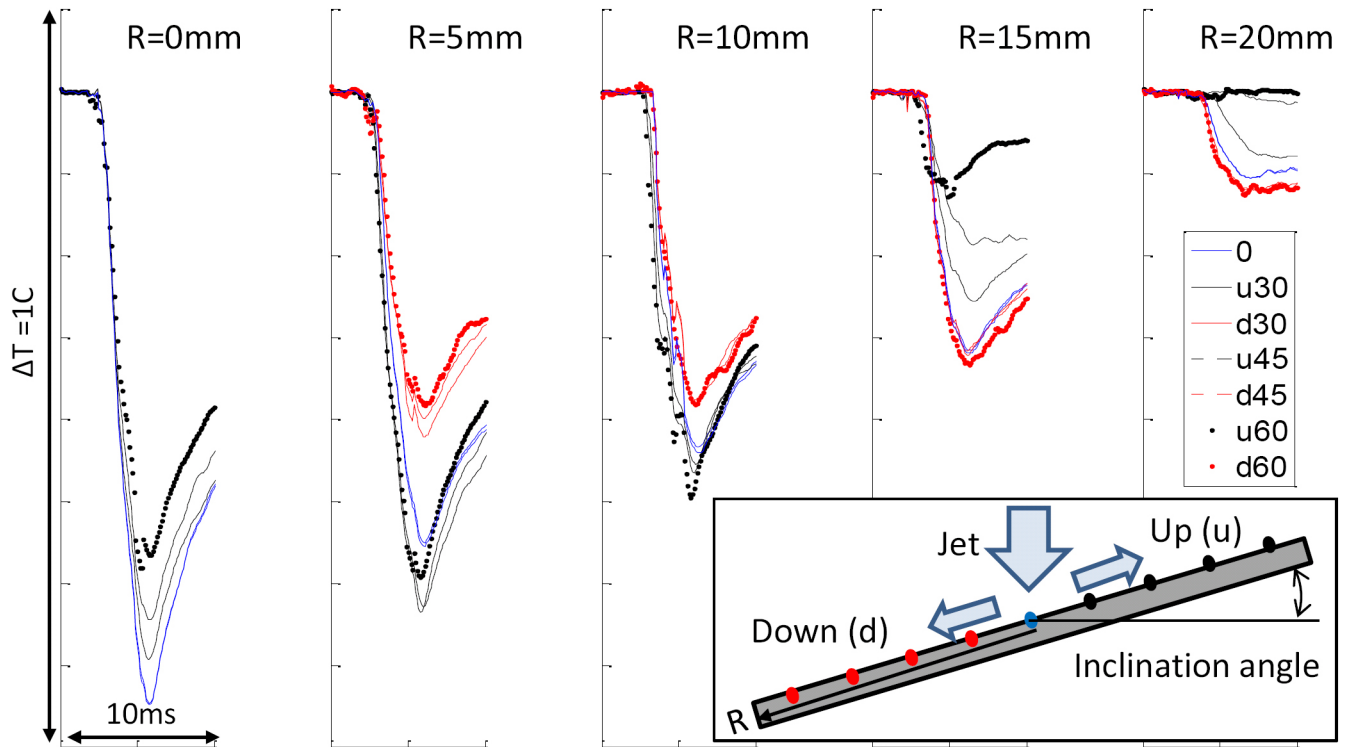


Figure 9. Thermocouple experimental results. Temperature variation as function of time at different locations.

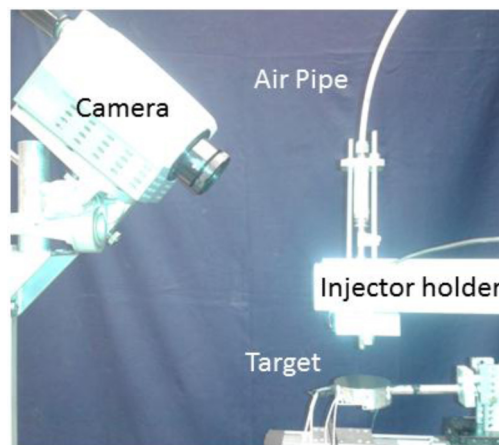


Figure 10. Thermal camera setup. The apparatus is placed in a black enclosure during the experiment to minimize the effects of the radiation from the surrounding.

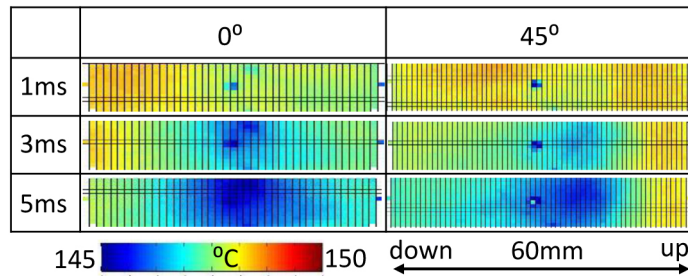


Figure 11. Example of thermal camera unprocessed results. Target surface temperature at different angles at different times.

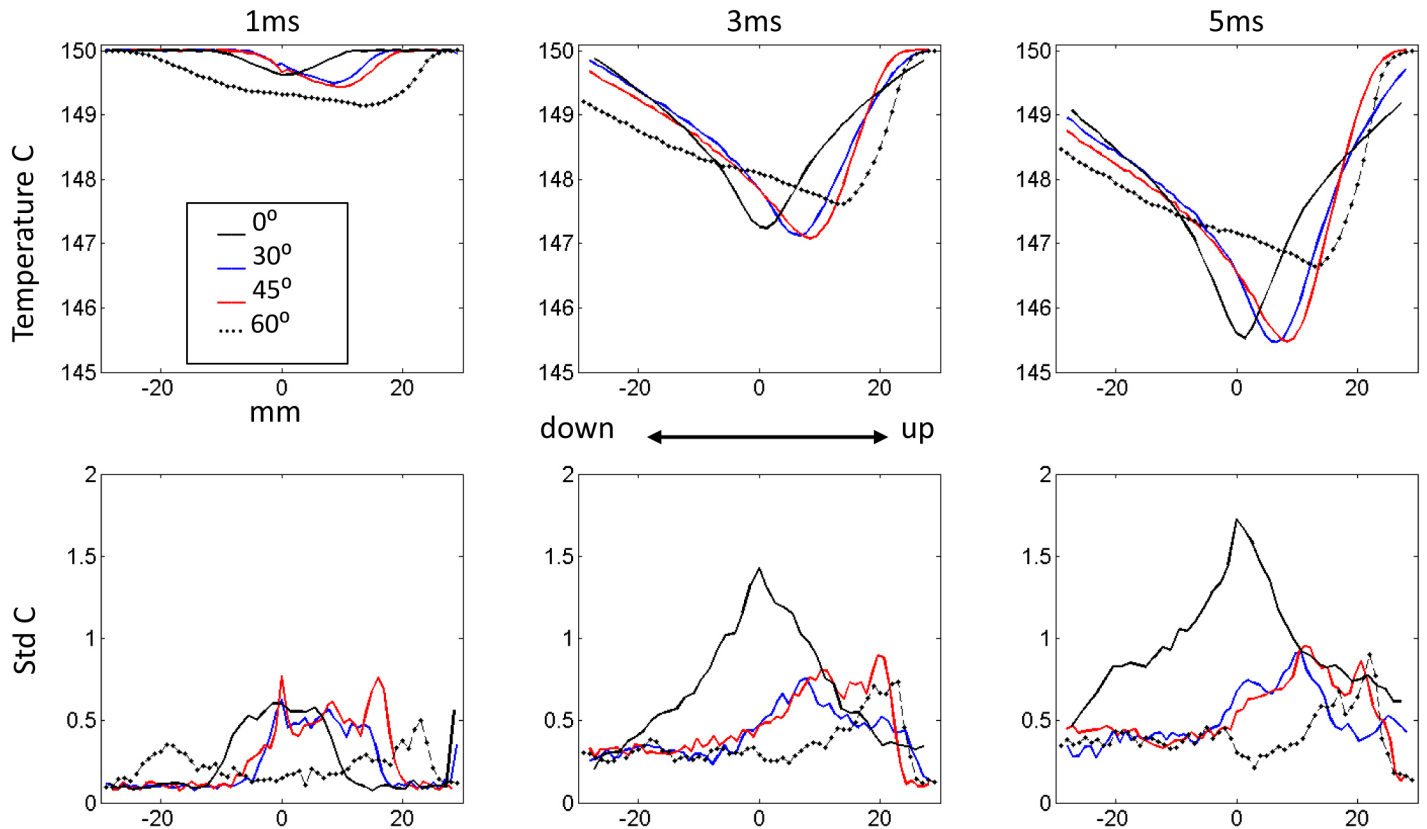


Figure 12. Thermal camera results in the line across the stagnation point as function of the position at different times. Top, average temperature of 20 samples at different times. Bottom, standard deviation of the same data.

MODELING METHODOLOGY

The CFD model is set up and run with the commercial code Star-ccm+ 7.02 by CD-Adapco following the general procedures described in the product user guide [40] and [19] for the specific impinging jet simulation.

LES (Large Eddy Simulation) is used as turbulence model for the study. This model basically consists on the full time-space resolution of the larger, energy carrying turbulent structures [40]. LES is highly computational expensive due to requisite of a large mesh size. Nowadays the application of LES is rapidly growing mainly due to the improvement in computer technology. The ability of this method to accurately capture impinging jet flow features and heat transfer characteristics is

studied in [19] and compared with more popular turbulence models such U-RANS (Unsteady-Reynolds Averaged Navier-Stokes). LES requires a sub grid model to account for the effects of the turbulent scales with length smaller than the mesh cell size. In this work the WALE (Wall Adapting Local Eddy viscosity) [42] sub-grid model is chosen as implemented in Star-ccm+ 7.02. This sub-grid model is particularly developed to account for the local effects of the wall on the flow, which is at the core of impinging jet simulation.

The computational domain for the case at 45° inclination is presented in Figure 13. The mesh counts a total of ~5E6 cells. Identical meshing strategy is used for all cases for consistent cross comparison of the results. The inlet boundary

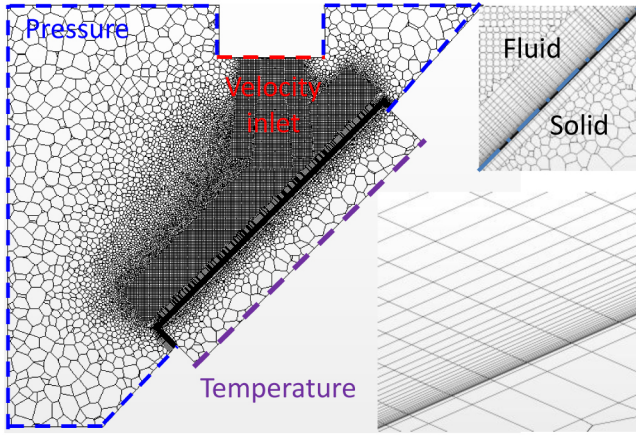


Figure 13. Example of computational mesh (45°) and boundary location.

is wider than the region interested by the jet by a good margin. The mesh is refined in the free jet and the wall-jet region. The target wall includes part of the solid to capture the effect of conjugate heat transfer. 20 prism layers grow from the solid-fluid interface, the first of which is thin enough to ensure a $y^+ < 1$ in every wall cell for the entire simulation, a basic requirement for this type of simulations [19]. Five prism layers grow into the solid domain. The mesh interface between the solid and fluid domain is fully conformal, which is essential to capture correctly heat transfer.

Figure 13 shows the location of the simulation boundaries. At the solid domain is applied a constant temperature boundary and the solid domain is initialized at the same temperature (150C). The other fluid boundaries are set to pressure.

The condition at the inlet boundary is the time resolved velocity profile measured with the PIV experiment. The measured profile is compared to the simulation results from a single-hole diesel spray model. The results of this comparison were previously discussed and graphically presented in Figure 2. At the nozzle the jet starts to exchange momentum with the surrounding by the entrainment of the surrounding fluid. The PIV measurements capture the result of all jet effects, thus including entrainment. The location of the inlet for the simulation is chosen so that compressibility effects are negligible (i.e. Mach number $Ma < 0,3$) this implies that the jet momentum is fully defined by the velocity field and that expansion shock waves are not present. Accordingly the simulations are run as incompressible. For a given time, the velocity profile is the result of the average of 100 samples. This practically results in a dampened size and magnitude of the vortex created by the jet leading edges (as discussed in the PIV section). A side simulation shows that the lead vortex self-generates rapidly and it is not necessary to resolve it if the inlet is sufficiently far from the target. The synthetic eddy method [41] available in Star-ccm+ allows to map representative isotropic turbulent structures at the inlet based on a length-time scale. This is included in the simulation.

However, the most important source of turbulence is generated in the growing shear layer. This turbulence source is resolved by the LES model [19].

The results of the CFD simulations are presented in terms of heat transfer coefficient h , based on the flow bulk temperature T_b by the correlation

$$h = \frac{q}{(T_w - T_b)} \quad (1)$$

where q and T_w are respectively the specific heat flux and the temperature of the wall cell.

In Figure 14 it is possible to follow the time-space evolution of the heat transfer coefficient. In the stagnation zone the boundary layer thickness is zero and a laminar boundary layer develops resulting in a smooth variation of the heat transfer coefficient. The boundary layer grows in thickness and eventually undergoes transition to turbulent. This evolution can be clearly observed comparing the results at 2ms and 3ms. The transition has a different character and shifts downstream with time. The term “transition” in this study refers to a change from a laminar-like to a turbulent-like flow. It is arguable whether the transition shown for 2ms can be compared with the canonical definition of transition in a boundary layer developing in space [35] (this case is a space-time evolution).

In Figure 14 it is also possible to compare the effect of different target angles on the heat transfer coefficient location and magnitude. Increasing the angle the stagnation shifts further up on the target. The jet has the strongest effects for the 0° and the 90° edge cases reaching values over 900W/m²K.

RESULTS - SINGLE PULSE IMPINGING JET EVOLUTION

Cross comparing the results obtained using different investigation methods on the same events it is possible to study and understand the evolution of the single pulse impinging jet with a depth otherwise unlikely to achieve.

In the PIV results at 0,75ms it is possible to see how the jet penetration rate differs between different target inclinations. If the target is inclined, even slightly, two effects occur. While the jet is approaching the fluid in front of it has to be displaced and with an angle this motion is facilitated. When the jet tip reaches the target its momentum is better aligned with the target surface. Consequently a preferential flow direction establishes and the wall-jet speed is higher.

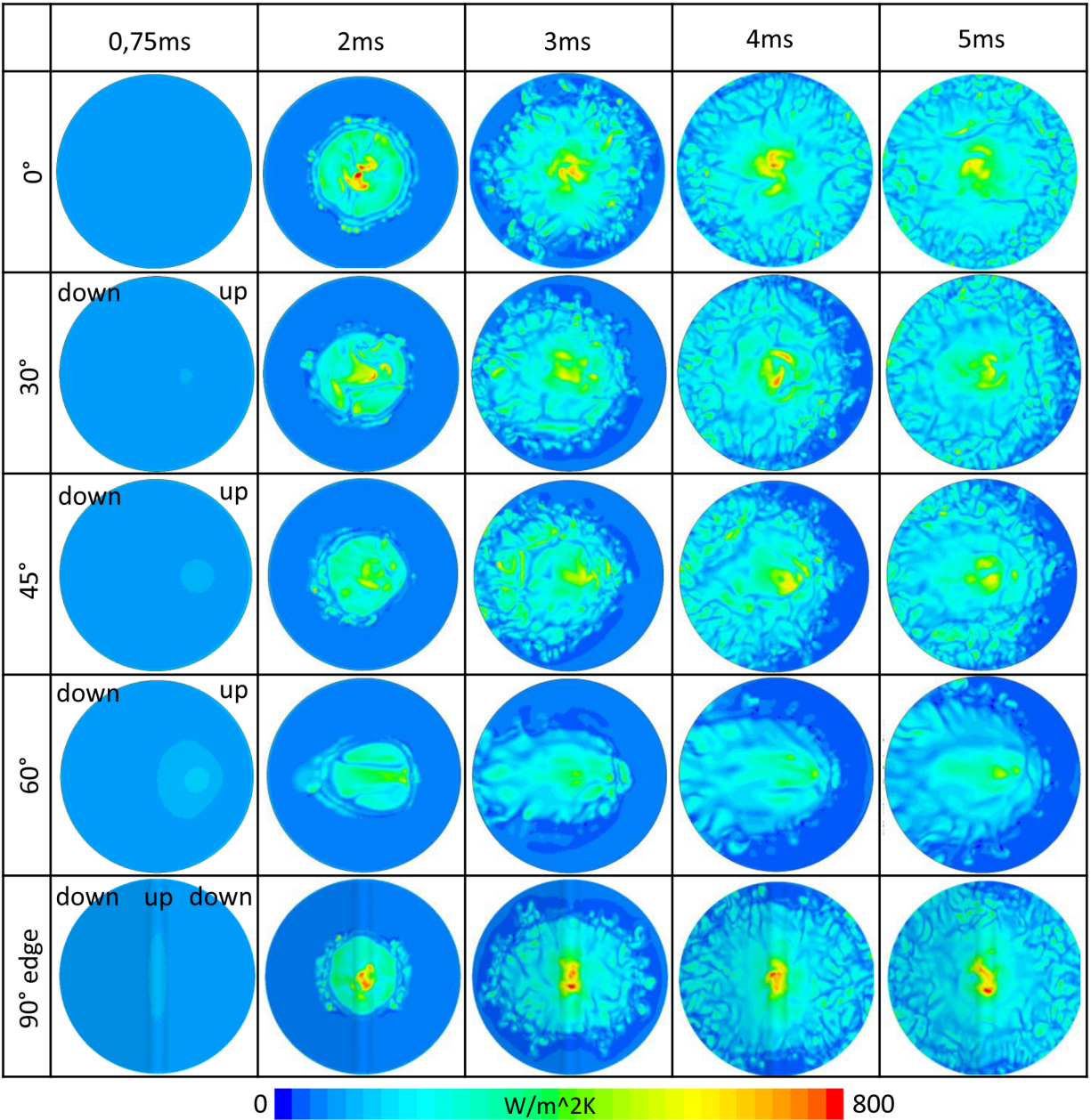


Figure 14. Heat transfer coefficient at different angles at different times. View normal to the target surface.

The results regarding the jet thermal interaction with the target (temperature and heat transfer coefficient) confirm the finding above. The jet first interacts with the wall after about 0,75-1ms from star of injection. Effects of the fact that the jet penetrates faster when approaching an inclined surface can be seen in the experimental results in [Figure 12](#) top. At time 1ms the case at 60° experienced a temperature change twice as the case at 0°, this indicates that the jet has been interacting with the surface for a longer time. The same behavior is captured also in the simulations where for the case at 0° and 0,75ms there is yet no interaction between the jet and the target differently than for all other target inclinations ([Figure 14](#)).

For the case 90° rounded edge, the jet is approaching the target edge in normal direction as in the 0° case. On the other hand, the inclination of the surfaces at the sides allows the jet front penetrate more easily with timing similar to those of the inclined flat surfaces ([Figure 14](#)).

[Figure 7](#) reports the average for the PIV results, here it is possible to notice that the jet approaching the target at 0° presents pronounced curvatures as opposed to the ones approaching an inclined surface. Furthermore, the standard deviation of the temperature measurements presented in [Figure 12](#) bottom is considerably higher for the 0° inclination. These facts indicate that with no preferential direction given

by an inclined surface the variation between consecutive jets is considerably higher.

The highest thermal effect is observed for the target at 0° but this occurs after a longer delay from start of injection. The results from the thermal camera in [Figure 12](#) clearly show that with the target at 0° inclination the jet thermal effect is more concentrated. Moreover, for this case the change in temperature change between 1ms and 5ms is the largest confirming that this configuration has the highest heat transfer coefficient. All cases in [Figure 12](#) show a similar temperature distribution with exception of the 60° case. This phenomenon is also captured by the CFD simulation where there is a clear difference in the turbulent structures between the case at 45° and 60° indicating a significant change in flow features. For the 90° edge the thermal interaction in the stagnation region is of similar magnitude than the 0° configuration, probably because in this region the jet undergoes similar lateral acceleration in the stagnation zone causing comparable heat transfer effects.

Inclining the target there is a shift of the stagnation zone upwards, this is clear in the results presented in [Figure 12](#). The jet encounters more resistance moving upwards due to the larger change in direction. As a result the wall-jet develops with higher speed and intensity downwards. This can be clearly seen in [Figure 9](#) with the red lines overtaking the black ones between $R=10$ and $R=15$. In the same figure it is possible to see that the jet has no effect for $R=20$ with a 60° inclination, meaning that the wall-jet never reaches this location. This agrees with the results in [Figure 12](#) and it is also captured correctly by the CFD simulations ([Figure 14](#))

All methods capture the pulse impinging jet features and trends very well and allows for a meaningful cross comparison. The most significant discrepancy is between the temperature measured with the thermal camera and the thermocouples with a maximum temperature difference during the injection of $\sim 5C$, $\sim 0.8C$ respectively this is easily explainable by the fact that in the thermal camera experiment the target is painted with a black coating that has significant thermal effect. This coating is necessary for an accurate measurement.

SUMMARY/CONCLUSIONS

The primary purpose of this work is to follow and understand the evolution of a single pulse impinging jet with characteristics relevant to diesel injection. The evolution of the same jet event is measured and modeled with different methods. The cross comparison simultaneously validates the different investigation methods and ease the understanding of the phenomena.

The penetration rate of the jet is affected by the target angle in two ways. To reach the target, firstly the jet needs to displace part of the fluid between its front and the wall. Secondly the free jet changes direction to create the wall-jet. Both these phenomena are facilitated with an inclined surface

establishing a preferential direction for the jet evolution. The impingement zone is found to move upwards with inclined target. A noticeable change in the wall-jet turbulent characteristics is found changing the target angle between 45° and 60° . The strongest thermal effect is found for the jet interacting with a normal surface. Nonetheless, it has to be considered that this interaction begins with a time delay that could be significant considering ICE injection timing.

The target with 90° rounded edge shares characteristics with both inclined and normal target orientation. Respectively, the jet flow develops faster and still maintains high thermal interaction at the impingement zone. This results in a high and localized thermal load. This type of geometry is present on the top part of modern diesel pistons and it is a known location of mechanical failure due to high thermally induced stresses. This work might help explaining this phenomenon.

Besides bringing further understanding on the evolution of pulse impinging, jet this work validates to an extent the ability of CFD simulation to predict this type of flows. CFD simulation are rapidly improving and becoming an indispensable tool in modern ICE development. This work can be useful in the development of these simulations when particular interest is devoted to the fluid-wall interaction.

AKNOWLEDGMENTS

The authors would like to warmly thank all the persons which cooperated in the execution of this work contributing with incomparably high specialist expertise. In particular Maxim Golubev for the execution of the PIV measurements and Eugenio De Benito Sienes.

REFERENCES

1. Jambunethan K., Lai E., Moss M. A. and Button B. L. [1992], A review of heat transfer data for single circular jet impingement, *Int. J. Heat and Fluid Flow*, Vol. 13, No. 2 106-115
2. Viskanta R. [1993], Heat transfer to impinging isothermal gas and flame jets. *Experimental Thermal and Fluid Science* 6:111-134
3. Baughn, J. W. and Shimizu, S. [1989], Heat transfer measurements from a surface with uniform heat flux and an impinging jet, *ASME J. Heat Transfer* 111/1097.
4. Cooper, D., Jackson, D. C., Launder, B. E. & Liao, G. X. 1993 Impinging jet studies for turbulence model assessment-I. Flow-field experiments. *Int. J. Heat Mass Transf.* 36, 2675-2684.
5. Katti, V. and Prabhu, S.V. [2008], Experimental study and theoretical analysis of local heat transfer distribution between smooth flat surface and impinging air jet from a circular straight pipe nozzle, *Int. J. Heat Mass Transfer* article in press.

6. Lytle, D. and Webb, B.W. [1994], Air jet impingement heat transfer at low nozzle plate spacings, *Int. J. Heat Mass Transfer* 37 1687-1697.
7. Gao, N., Sun H. and Ewing D. [2003], Heat transfer to impinging round jets with triangular tabs, *Int. J. Heat Mass Transfer* 46 2557-2569.
8. O'Donovan T. S. and Murray D. B. [2007], Jet impingement heat transfer - Part I: Mean and root-mean-square heat transfer and velocity distributions, *Int. J. Heat and Mass Transfer* 50 3291-3301.
9. O'Donovan T. S. and Murray D. B. [2007], Jet impingement heat transfer - Part II: A temporal investigation of heat transfer and local fluid velocities, *Int. J. Heat and Mass Transfer* 50 3302-3314.
10. Gao N. and Ewing D. [2006], Investigation of the effect of confinement on the heat transfer to round impinging jets exiting a long pipe, *Int. J. of Heat and Fluid Flow* 27 33-41
11. Koseoglu M.F. and Baskaya S. [2007], The effect of flow field and turbulence on heat transfer characteristics of confined circular and elliptic impinging jets, *Int. J. of Thermal Sciences* article in press.
12. Bovo M., Davidson L., "On the transient modelling of impinging jets heat transfer. A practical approach." proceedings, *Turbulence, Heat and Mass Transfer 7*, Palermo.
13. Yang Yue-Tzu, Tsai Shiang-Yi [2007], Numerical study of transient conjugate heat transfer of a turbulent impinging jet. *Heat and Mass Transfer* 50 799-807.
14. Lien, F.S., Chen, W.L. and Leschziner, M.A. [1996], Low-Reynolds-Number Eddy-Viscosity Modelling Based on Non-linear Stress-Strain/Vorticity Relations, *Proc. 3rd Symp. on Engineering Turbulence Modelling and Measurements*, Crete, Greece.
15. Angioletta M., Ninoa E., Ruocob G., CFD turbulent modelling of jet impingement and its validation by particle image velocimetry and mass transfer measurements, *International Journal of Thermal Sciences* 44 (2005) 349-356
16. Bovo M. et al, On the numerical modelling of impinging jet heat transfer, *Int. Symp. on Convective Heat and Mass Transfer in Sustainable Energy*, 2009, Tunisia
17. Hofmann H. M., Kaiser R., Kind M., martin H., Calculations of steady and pulsating impinging jets-an assessment of 13 widely used turbulence models, *Numerical heat transfer, part b*, 51: 565-583, 2007.
18. Hällqvist Thomas 2006, Large Eddy Simulation of Impinging Jets with Heat Transfer KTH Mechanics, SE-100 44 Stockholm, Sweden, dissertation thesis.
19. Bovo Mirko & Davidson Lars (2013), On the Numerical Modeling of Impinging Jets, *Heat Transfer-A Practical Approach, Numerical Heat Transfer, Part A: Applications: An International Journal of Computation and Methodology*, 64:4, 290-316.
20. Husberg, T., Gjirja, S., Denbratt, I., Omrane, A. et al., "Piston Temperature Measurement by Use of Thermographic Phosphors and Thermocouples in a Heavy-Duty Diesel Engine Run Under Partly Premixed Conditions," *SAE Technical Paper* [2005-01-1646](#), 2005, doi: [10.4271/2005-01-1646](#).
21. Sirignano William A., *Fluid Dynamics of Spray - 1992 Freeman Scholar Lecture. Journal of Fluids Engineering*, 1993 Vol. 115/345.
22. Naber, J. and Siebers, D., "Effects of Gas Density and Vaporization on Penetration and Dispersion of Diesel Sprays," *SAE Technical Paper* [960034](#), 1996, doi: [10.4271/960034](#).
23. Siebers D., "Liquid-Phase Fuel Penetration in Diesel Sprays," *SAE Technical Paper* [980809](#), 1998, doi: [10.4271/980809](#).
24. Abraham, J., "What is Adequate Resolution in the Numerical Computations of Transient Jets?," *SAE Technical Paper* [970051](#), 1997, doi: [10.4271/970051](#).
25. Abani Neerev, reitz Rolf D., Modeling sub grid scale mixing of vapor in diesel spray using jet theory, *ICLASS 2009, 11th Triennial International Annual Conference on Liquid Atomization and Spray Systems*, Vail, Colorado USA.
26. Wang, Y., Ge, H., and Reitz, R., "Validation of Mesh- and Timestep- Independent Spray Models for Multi-Dimensional Engine CFD Simulation," *SAE Int. J. Fuels Lubr.* 3(1):277-302, 2010, doi: [10.4271/2010-01-0626](#).
27. Park Sung Wook, Reitz Rolf D., A gas jet superposition model for CFD modeling of group-hole nozzle sprays, *Volume 30, Issue 6, December 2009, Pages 1193-1201*.
28. Kösters, A. and Karlsson, A., "A Comprehensive Numerical Study of Diesel Fuel Spray Formation with OpenFOAM," *SAE Technical Paper* [2011-01-0842](#), 2011, doi: [10.4271/2011-01-0842](#).
29. Azevedo L. F. A., Webb B. W. Queiroz M., Pulsed Air Jet Impingement Heat Transfer Experimental Thermal and Fluid Science, 1994; 8:206-213
30. Janetzke Timm, Nitsche Wolfgang, Time resolved investigations on flow field and quasi wall shear stress of an impingement configuration with pulsating jets by means of high speed PIV and a surface hot wire array *International Journal of Heat and Fluid Flow* 30 (2009) 877-885.
31. Xu Peng, Yu Boming, Qiu Shuxia, Poh Hee Joo, Mujumdar Arun S., Turbulent impinging jet heat transfer enhancement due to intermittent pulsation, *International Journal of Thermal Sciences* 49 (2010) 1247-1252.
32. Hofmann Herbert Martin, Movileanu Daniela Luminita, Kind Matthias, Martin Holger, Influence of a pulsation on heat transfer and flow structure in submerged impinging jets, *International Journal of Heat and Mass Transfer* 50 (2007) 3638-3648.
33. Song, L. and Abraham, J., "Influence of Wall Impingement on the Structure of Reacting Jets," *SAE Technical Paper* [2003-01-1042](#), 2003, doi: [10.4271/2003-01-1042](#).

34. Pickett, L. and López, J., "Jet-Wall Interaction Effects on Diesel Combustion and Soot Formation," SAE Technical Paper [2005-01-0921](#), 2005, doi:[10.4271/2005-01-0921](#).
35. Hinze J. O., Turbulence, ISBN 0-07-029037-7
36. Baert, R., Klaassen, A., and Doosje, E., "Direct Injection of High Pressure Gas: Scaling Properties of Pulsed Turbulent Jets," *SAE Int. J. Engines* 3(2):383-395, 2010, doi:[10.4271/2010-01-2253](#).
37. Raffel M., Willert C. & Kompenhans J., Particle Image Velocimetry, A Practical Guide. Springer, 1998. 253 pp. ISBN 3540 63683 8.
38. Product Information Coaxial Surface Thermocouple Probes, Medtherm Corporation, Huntsville, Alabama USA
39. Osso C. Arroyo, (2009) "Aerothermal Investigation of an Intermediate Duct", Thesis for the Degree of Doctor of Philosophy, Chalmers University of Technology.
40. Star-ccm+ 7.04.011 userguide by CD-Adapco.
41. Jarrin N., Benamadouche S., Laurence D., and Prosser R.. 2006. "A synthetic-eddy-method for generating inflow conditions for large eddy simulations". *International Journal of Heat and Fluid Flow*, 27, pp. 585-593.
42. Nicoud, F. and Ducros, F., 1999. "Subgrid-Scale Stress Modelling Based on the Square of the Velocity Gradient Tensor," *Flow, Turbulence and Combustion*, 62, pp. 183-200.

The Engineering Meetings Board has approved this paper for publication. It has successfully completed SAE's peer review process under the supervision of the session organizer. This process requires a minimum of three (3) reviews by industry experts.

All rights reserved. No part of this publication may be reproduced, stored in a retrieval system, or transmitted, in any form or by any means, electronic, mechanical, photocopying, recording, or otherwise, without the prior written permission of SAE.

ISSN 0148-7191

Positions and opinions advanced in this paper are those of the author(s) and not necessarily those of SAE. The author is solely responsible for the content of the paper.

SAE Customer Service:

Tel: 877-606-7323 (inside USA and Canada)

Tel: 724-776-4970 (outside USA)

Fax: 724-776-0790

Email: CustomerService@sae.org

SAE Web Address: <http://www.sae.org>

Printed in USA